

Template-Free Growth of High-Temperature Superconductor Nanowires

Potticary, Jason; Luke, Emily J.; Christodoulou, Ektor M. S.; Davies, Rowena; Haughton, Sorrel; Feuillet-Palma, Cheryl; Recoba-Pawłowski, Eliana; Leridon, Brigitte; Griffin, Sarah; Hall, Simon R.

DOI:

[10.1002/ssr.202300087](https://doi.org/10.1002/ssr.202300087)

License:

Creative Commons: Attribution (CC BY)

Document Version

Publisher's PDF, also known as Version of record

Citation for published version (Harvard):

Potticary, J, Luke, EJ, Christodoulou, EMS, Davies, R, Haughton, S, Feuillet-Palma, C, Recoba-Pawłowski, E, Leridon, B, Griffin, S & Hall, SR 2023, 'Template-Free Growth of High-Temperature Superconductor Nanowires', *Small Structures*. <https://doi.org/10.1002/ssr.202300087>

[Link to publication on Research at Birmingham portal](#)

General rights

Unless a licence is specified above, all rights (including copyright and moral rights) in this document are retained by the authors and/or the copyright holders. The express permission of the copyright holder must be obtained for any use of this material other than for purposes permitted by law.

- Users may freely distribute the URL that is used to identify this publication.
- Users may download and/or print one copy of the publication from the University of Birmingham research portal for the purpose of private study or non-commercial research.
- User may use extracts from the document in line with the concept of 'fair dealing' under the Copyright, Designs and Patents Act 1988 (?)
- Users may not further distribute the material nor use it for the purposes of commercial gain.

Where a licence is displayed above, please note the terms and conditions of the licence govern your use of this document.

When citing, please reference the published version.

Take down policy

While the University of Birmingham exercises care and attention in making items available there are rare occasions when an item has been uploaded in error or has been deemed to be commercially or otherwise sensitive.

If you believe that this is the case for this document, please contact UBIRA@lists.bham.ac.uk providing details and we will remove access to the work immediately and investigate.

Template-Free Growth of High-Temperature Superconductor Nanowires

Jason Potticary, Emily J. Luke, Ektor M. S. Christodoulou, Rowena Davies, Sorrel Haughton, Cheryl Feuillet-Palma, Eliana Recoba-Pawłowski, Brigitte Leridon, Sarah Griffin, and Simon R. Hall*

As devices become ever smaller and more efficient, the crystallochemically controlled synthesis of high-performance materials that comprise their core has attracted enormous attention. Integration of complex functional materials into the next generation of electronic devices will require exquisite control of anisotropic form, either as nanotubes, nanotapes, or nanowires, yet the easy preparation of abundant quantities of them remains stubbornly challenging. Herein, a template-free, flux-mediated growth of vast quantities of three compositions of phase-pure, high-temperature superconductor nanowires, including for the first time, nanowires of the technologically important quinary superconductor $\text{Bi}_2\text{Sr}_2\text{CaCu}_2\text{O}_{8+x}$ (B2212) is demonstrated. The results of this work may provide an opportunity to investigate the physics and chemistry of highly anisotropic superconductor nanowires and enable their incorporation into nanoelectronics and energy generation systems.

applications in nanoelectronics, as sensors, and in energy devices.^[1–4] Nanostructures of more complex functional materials such as CuO, ZnO, and ternary oxides open up the possibility of devices such as those required for power generation, gas sensing, or solar cell technologies.^[5–7] Current nanowire syntheses of these materials can be via a top-down approach (e.g., etched from larger material), or bottom-up, via a vapor–liquid–solid (VLS) method, solution growth, or templating. For more advanced devices that require quaternary and quinary complex functional materials, however, the lack of a suitable catalytic nanoparticle and the preponderance of associate phase formation, means that these methods tend to fail badly when attempting the bulk syntheses of nano-

wires. What is required, therefore, is a method that can circumvent associate phase formation and yet facilitate nanowire growth. Here, we show just such a method, whereby synthetically simulating the intermediate (post 500 °C) structure of a biotemplated reaction mechanism using flux-mediated melting of quasi-catalytic nanoparticles, nanowires of quaternary and quinary superconductors can be grown in vast abundance. This result should, therefore, remove a significant block in the development of new technologies, as it has been shown, for example, that quinary high-temperature superconductors are capable of emitting radiation in the terahertz, frequency range.^[8] Being able to access huge quantities of quinary oxide nanowires, therefore, will unlock new applications in areas as diverse as wireless communication, state and personal security, medical diagnostics, and nondestructive testing of materials.^[9]

As devices become ever smaller and more efficient, the crystallochemically controlled synthesis of high-performance materials that comprise their core has attracted enormous attention. Integration of complex functional materials into the next generation of electronic devices will require exquisite control of anisotropic form, either as nanotubes, nanotapes, or nanowires, yet the easy preparation of abundant quantities of them remains stubbornly challenging. One method that has been used to create phase-pure nanowires of quaternary element high-temperature superconductors, is the microcrucible (MC) growth mechanism. This is a bottom-up approach that involves a nano-sized “crucible” of a liquid phase, rich in a specific ion that extrudes material from the solid matrix, in which it is situated.

1. Introduction


The development of electronic device complexity necessarily comes with challenges in the design and creation of new materials that form the core of these devices. Silicon nanowires, for example, have been actively researched for decades, finding

J. Potticary, E. J. Luke, E. M. S. Christodoulou, R. Davies, S. Haughton, S. R. Hall

Complex Functional Materials Group
School of Chemistry
University of Bristol
Bristol BS8 1TS, UK
E-mail: simon.hall@bristol.ac.uk

C. Feuillet-Palma, E. Recoba-Pawłowski, B. Leridon
Physics and Materials Laboratory (LPEM)
ESPCI Paris – PSL
75005 Paris, France

S. Griffin
School of Chemistry
University of Birmingham
Edgbaston B15 2TT, Birmingham, UK

 The ORCID identification number(s) for the author(s) of this article can be found under <https://doi.org/10.1002/ssstr.202300087>.

© 2023 The Authors. Small Structures published by Wiley-VCH GmbH. This is an open access article under the terms of the Creative Commons Attribution License, which permits use, distribution and reproduction in any medium, provided the original work is properly cited.

DOI: 10.1002/ssstr.202300087

In our previous work, the MC mechanism was observed directly.^[10] In more detail, the MC migrates through the surrounding solid matrix and reaches the surface of material. When the MC reaches the surface of the matrix, a flux (in this case sourced from the sodium alginate biopolymer) depresses the melting point, thereby, forming a liquid crucible on the surface of the material. In this crucible, precursors can mix and form a thermodynamically stable crystal that is extruded out from the precursor matrix in the form of a nanowire (Figure S1, Supporting Information). These wires are characterized by flat, faceted ends, and without tapering toward the end due to the nature of how they grow. Our previous work has observed MC growth of yttrium barium copper oxide (Y_2BaCuO_5) nanowires, facilitated by molten nanoparticles of BaCO_3 , surrounded by a carbonaceous matrix containing Y and Cu oxides.^[10] The molten BaCO_3 nanoparticles act as a quasi-catalytic, morphological director of nanowire growth at high temperatures and produce single-crystal nanowires of the target phase. This method is a biopolymer-mediated approach, where a biopolymer is a common naturally occurring polymer—such as dextran or sodium alginate. These biopolymers can template to metal salts in solution, enabling better mixing of the metal ions when compared to solid-state syntheses. The nanowire yield via this method is generally low though and the decomposition of the biopolymer can lead to the generation of carbon dioxide within the furnace, leading to carbothermal reduction and/or the establishment of unwanted associate phases. From this initial work, it was determined that three principal criteria must be applied to induce the MC mechanism: a solid matrix comprising one or more of the precursor elements, nanoparticles to act as the MC, and a flux in which the nanoparticles can melt and react with the solid matrix around it, thereby, promoting nanowire growth.^[10] In that study, nanoparticles of barium carbonate acted as the MC, which were generated in situ via the decomposition of a biopolymer, providing a cocooning constraint on nanoparticle growth. However, not all inorganic material syntheses are compatible with a biopolymer-mediated approach, so a more general protocol to artificially induce this mechanism via a solid-state method was required. We note that in previously reported biotemplating of complex oxides, the biopolymers used commonly contained salts of the alkali metals sodium and potassium.^[11,12] Although not initially thought to play a role in the formation of nanowires, their function as a morphogenitor for anisotropy in metal oxide compounds has been speculated upon.^[13] In this work, therefore, we very simply introduce sodium in the form of NaCl to a nano-seeded reaction mixture as a high-temperature flux. To test this new template-free nanowire synthesis, we chose to apply the technique to $\text{YBa}_2\text{Cu}_3\text{O}_7$ (Y123), $\text{LaBa}_2\text{Cu}_3\text{O}_7$ (La123), and $\text{Bi}_2\text{Sr}_2\text{CaCu}_2\text{O}_8$ (Bi2212). Y123 was chosen due to the fact that the MC mechanism has previously been observed in this system, and has been observed in situ for Y_2BaCuO_5 . La123 was subsequently chosen as it is another rare-earth superconducting cuprate and would thus confirm whether this synthetic mechanism was more broadly applicable to other systems. Finally, Bi2212 was chosen due to its increased complexity of crystal structure over Y123 and La123, and also because single-crystal nanowires of this technologically important system are yet to be reported.

2. Results and Discussion

To apply these criteria to Y123, and thereby induce the MC mechanism, a synthesis from Y_2O_3 , CuO, BaCO_3 nanoparticles, and NaCl as a flux was devised. This was carried out utilizing a solid-state method, where the Y_2O_3 and CuO were grounded together with the barium carbonate nanoparticles and sodium chloride as a flux. To aid in the solid-state reaction, the precursor powders were compressed into a solid pellet prior to calcination. The synthesized BaCO_3 particles exhibited a mean diameter of 29.1 ± 1.3 nm, the size distribution, transmission electron microscopy (TEM), and powder X-ray diffraction (pXRD) of these particles can be seen in Figure S2, Supporting Information. Figure 1a shows scanning electron microscopy (SEM) analysis of the resultant surface of the pellet after calcination to 880°C with 10 wt% of NaCl. It can be clearly seen that fine wire-like structures are present in significant abundance. The width of the wires was 100.6 nm with a lognormal distribution, where $\ln\sigma = 0.363$. The direction of growth of the wires is generally outward from the surface of the pellet rather than parallel, which supports the theory that these are grown with the MC mechanism. The wires consistently exhibit a lack of tapering toward the end, without any evidence of a catalytic droplet, which also suggests that the wires are grown from the MC mechanism rather than the more commonly observed VLS mechanism.^[14] Interestingly, clusters of the wires appear to be growing from scattered nucleation points, some of which have shoulders indicative of flux-creep. This results in wires which have merged and exhibit stepped edges.^[10] Due to the abundance of wires obscuring their origins, it was difficult to characterize the range of lengths observed for the wires. The longest observed full wire which was not obscured by others was $\approx 8\ \mu\text{m}$, which had a width of 100 nm, resulting in an aspect ratio of 80. In each bulk sample, wires were easily isolated from the pellet material by sonication in ethanol for ≈ 10 s, which could then be deposited onto a TEM grid. Subsequent TEM and selected-area electron diffraction (SAED) studies confirmed that the nanowires observed were the target Y123 phase, with a zone axis of [001] (Figure 1b,c). TEM and pXRD of the BaCO_3 nanoparticles can be seen in Figure S2, Supporting Information. pXRD of the bulk pellet of Y123 can be seen in Figure S3, Supporting Information, as well as a distribution of measured widths of the wires.

Variable-temperature pXRD analysis (Figure 2) of the flux-assisted and template-free reaction mixture shows that crystalline NaCl is not present above 710°C , which is $\approx 100^\circ\text{C}$ lower than its typical melting point of 801°C .^[15] This depression of melting point suggests that the Na salt is forming a eutectic mixture with some of the other precursors and acting as a flux to help form liquid-phase intermediates at lower temperatures. This liquid phase may enable access to intermediate phases that differ from control experiments, allowing alternative reaction pathways that were otherwise unable to be reached. Interestingly, the target Y123 phase begins to form at a much lower temperature than expected (670°C) before transforming to the non-superconductive phase Y211, which begins at 790°C . Conventionally, a dwell temperature of $850\text{--}920^\circ\text{C}$ is utilized to synthesize Y123, but again, the molten salt eutectic allows the target phase to form at a much lower temperature.^[16] The pXRD data for this analysis were captured at 20°C intervals between 650 and 930°C and dwelled at

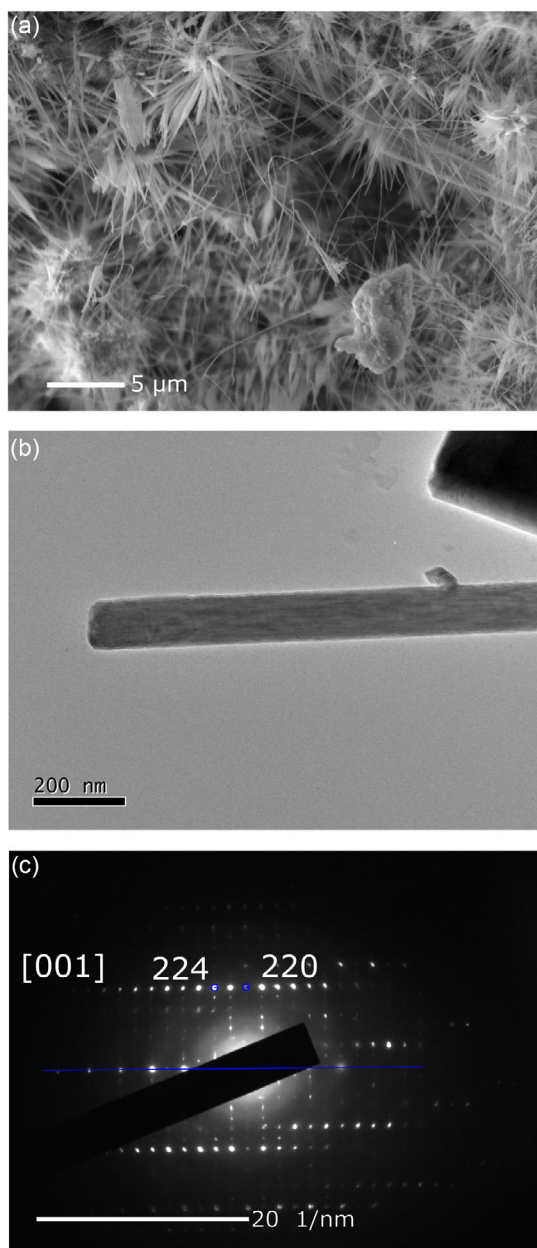


Figure 1. a) Scanning electron micrograph depicting a section of the Y123 nanowires grown through the flux-mediated synthesis. b) Transmission electron micrograph of a single wire from the same sample and c) selected area electron diffraction from the same wire. The zone axis was calculated to be [001].

these temperatures while the pXRD was obtained. As such, the overall experiment was much longer than would ordinarily take place which could have implications for the target phase formation being at much lower temperatures than expected, but it should also be noted that the depression of the melting point of NaCl is still occurring at much lower temperatures than would be typical.

This flux-mediated growth method was subsequently applied to $\text{LaBa}_2\text{Cu}_3\text{O}_7$ (La123) and $\text{Bi}_2\text{Sr}_2\text{CaCu}_2\text{O}_8$ (Bi2212) to determine if it was applicable to other cuprate superconductors.

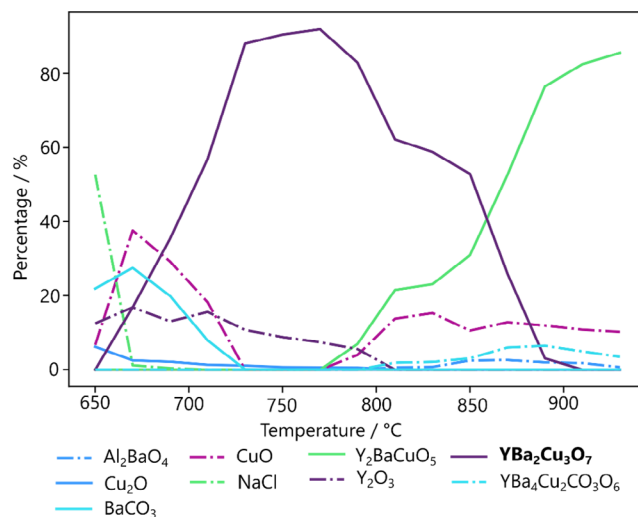


Figure 2. Phase evolution diagram as determined by Rietveld refinement of the variable-temperature pXRD experiments (Full data provided in Figure S4 and Table S1, Supporting Information). The data show that the Y123 phase begins to form at 670 °C, transforming into Y211 at 790 °C.

This is a sterner test than it seems, as the synthesis of Bi2212 nanowires has yet to be reported. Mechanistically, the mechanism of Bi2212 “whisker” growth has been previously suggested to occur through the MC mechanism,^[17] and so the system should at least be compatible with the MC growth mechanism observed previously and here for Y123.

The synthesis of La123 was carried out in a similar vein to the Y123 synthesis, with BaCO_3 nanoparticles added to a solid-state mixture of CuO and La_2O_3 , along with NaCl to act as a flux. Dwell temperatures between 660 and 880 °C with 10 °C increments were studied, each with 2-hour dwell times. Nanowires were observed at several temperatures: between 810–830 °C and at 860 °C. These wires were abundant and were found to grow from different morphological regions throughout the sample, with observations of wires growing from blocky sections of material as well as areas with a less well-defined shape. The data presented in Figure 3 show SEM, TEM, and SAED of samples grown at 820 °C with a 2 h dwell time and 10% of NaCl flux. It can be seen from Figure 3a that the sample exhibits numerous wires growing from a blocky region of the material. These wires were found to exhibit a range of diameters between 200 and 30 nm, with an average diameter of 96 nm (Figure S5, Supporting Information). The distribution of wire widths was wide in this case, with a standard deviation of 41 nm. SAED (Figure 3c) from a single wire was indexable to $\text{LaBa}_2\text{Cu}_3\text{O}_7$ with a zone axis of $[3\bar{3}2]$ using CrysTBox software for analysis.^[18]

In the case of Bi2212, the synthetic protocol needed to be adapted due to it being a quinary metal oxide. To prevent the necessity for a reaction between five individual components, mixed-metal oxides were utilized. In this case, inspiration was drawn from a previous study, where the phase evolution of Bi2212 was examined. $\text{Bi}_2\text{Sr}_2\text{CuO}_6$ (Bi-2201), copper oxide, and a mixed strontium-bismuth-calcium oxide phase were determined to be important precursors in the synthesis via biopolymer-mediated growth.^[19] To emulate this, we chose to

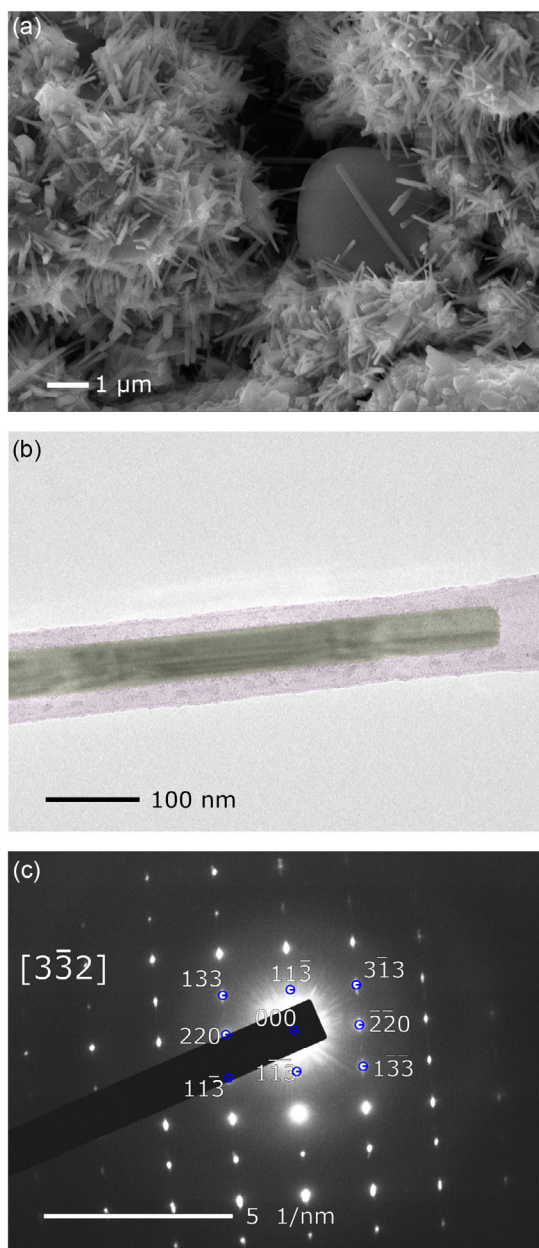


Figure 3. a) Scanning electron micrograph depicting a section of the La123 nanowires grown through the flux-mediated synthesis. b) Transmission electron micrograph of a wire from the same sample and c) selected area electron diffraction from the same wire. The zone axis was calculated to be $[3\bar{3}2]$. False color has been added to (b) to distinguish the La123 nanowire from the lacy carbon on which it is resting.

use calcium copper acetate hexahydrate and Bi-2201 as the precursors for Bi2212, along with NaCl as a flux. Due to the necessity for noncongruent crystallization in the synthesis of $\text{CaCu}(\text{OAc})_4 \cdot 6\text{H}_2\text{O}$, it was not possible to employ the same nanoparticle synthesis for this compound. Therefore, larger crystals of $\text{CaCu}(\text{OAc})_4 \cdot 6\text{H}_2\text{O}$ were first grown before subsequent ball-milling into smaller particles. The majority of these particles were found by SEM to be larger than one micron, but it was

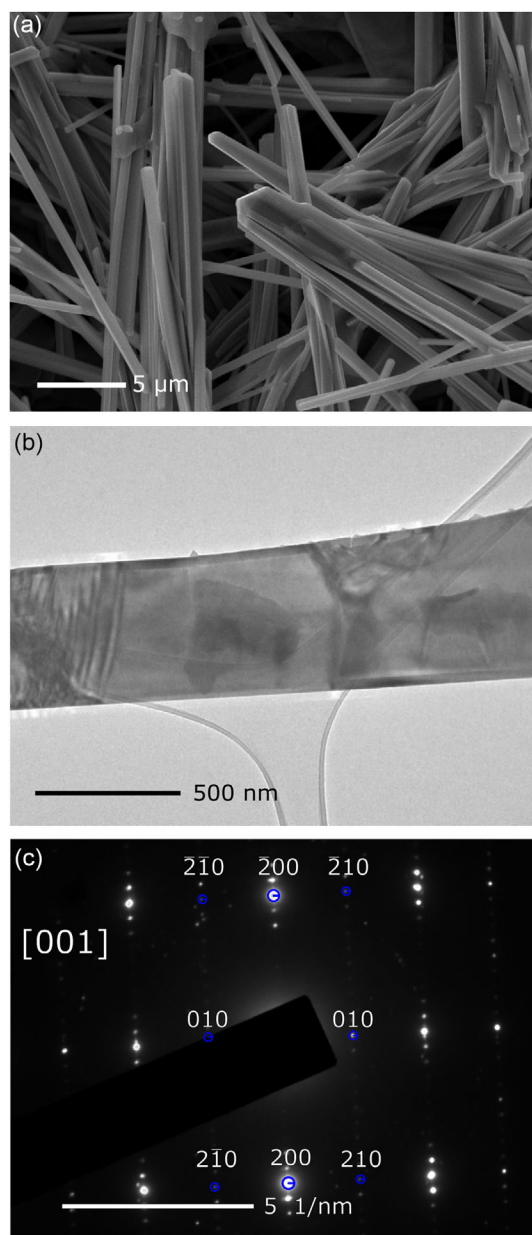


Figure 4. a) Scanning electron micrograph depicting a section of Bi2212 nanowires grown through the flux-mediated synthesis. b) Transmission electron micrograph of a wire from the same sample and c) selected area electron diffraction from the same wire. The zone axis was calculated to be $[001]$.

observed by TEM, smaller crystallites were present, with a mean particle diameter of 540 nm (Figure S6, Supporting Information, contains the analysis of these particles). While these particles were determined not to be as small as the BaCO_3 particles synthesized for the YBCO and La123 syntheses, it was reasoned that there would be small enough crystallites for a proof-of-concept examination of the growth of Bi2212 nanowires.

After synthesis at 850 °C with a 2-h dwell time and 30% NaCl with respect to bismuth, the resulting pellet exhibited many clusters of nanowires. In contrast to the Y123 and La123 syntheses,

the Bi2212 nanowires were much wider an average width of 570 ± 1.40 nm (Figure S7, Supporting Information), which is consistent with the theory that the nanoparticles are behaving as a microcrucible. As the $\text{CaCu}(\text{OAc})_4 \cdot 6\text{H}_2\text{O}$ particles are larger than the BaCO_3 particles, the microcrucible for this synthesis is larger and thus the wires are wider. TEM and SAED were performed on the sample (Figure 4). SAED of the wires determined that they were indexable to the target phase with a zone axis of [001]. However, the SAED was also indexable to Bi2201, and subsequent EDX analysis (Figure S8, Supporting Information) indicated that the material was deficient in calcium. It is likely, therefore, that the phase present is an off-stoichiometry form of Bi2212 with a calcium content between that of Bi2201 and Bi2212. It was noted that this synthesis was unsuccessful when the Bi2201 was synthesized via an alternative method, such as using a natural deep eutectic solvent as carried out initially by Rojas et al.^[20] This indicates that the shape and size of the crystallites in the Bi2201 precursor are integral for the subsequent synthesis. It is possible that for this system, it is the Bi2201

precursor that is behaving as the nanoparticulate material instead of the $\text{CaCu}(\text{OAc})_4 \cdot 6\text{H}_2\text{O}$, but in situ, observation of the nanowire growth would be required to determine if this is the case.

For La123 nanowires, EDX showed that the composition in some cases was lanthanum deficient (Figure S9, Supporting Information), whereas, in the case of Y123, the elemental weight percentage was as expected (Figure S10, Supporting Information).

To further show the structure of the nanowires, additional TEM data are presented in Figure S11, Supporting Information.

Finally, to confirm the superconductive properties of the bulk material, SQUID magnetometry was carried out on all three samples (Figure 5), by crushing the calcined pellets which comprised the bulk and the nanowires, and placing them into gel capsules. The Y123 and Bi2212 samples exhibited superconductivity at the expected critical temperatures of 86 and 80.5 K, respectively. Despite electron diffraction confirming the nanowires as La123, magnetometry of the bulk sample did not appear to show a superconducting transition, instead exhibiting an upturn

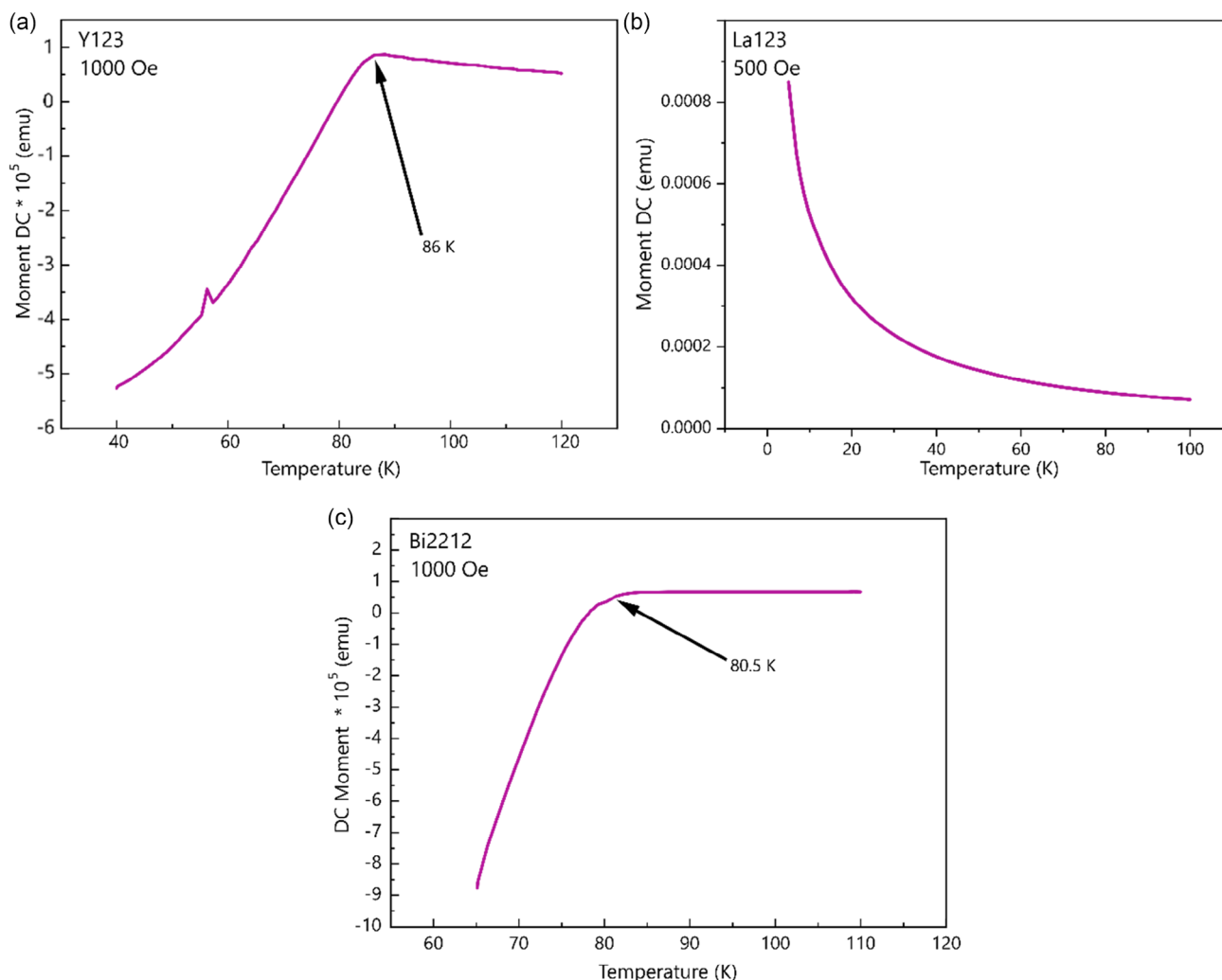


Figure 5. a) Zero-field cooled measurements with an applied field of 1,000 Oe for the Y123 sample. This sample exhibits an onset T_c of 86 K. b) Zero-field cooled measurements with an applied field of 500 Oe for the La123 sample. The sample was found to exhibit paramagnetic behavior. c) Zero-field cooled measurements with an applied field of 1,000 Oe for the Bi2212 sample. The sample was found to exhibit an onset T_c of 80.5 K.

characteristic of a paramagnetic sample. It is likely that in this case the signal occurring due to impurity phases was obscuring the superconducting transition, or that the La123 phase was not optimally oxygenated, resulting in no superconducting behavior. Oxygen annealing steps could therefore be utilized on the pellet to further sharpen the superconducting transition, however, this goes beyond the scope of the present work. As this is for a bulk technique, we cannot confirm from these data that the wires themselves are superconductive, but that there is some superconductive material within the pellet. Some attempts could be made to measure the resistance of the wires directly by contacting wires directly to the nanowires, but again this goes beyond the scope of the current work.

3. Conclusion

Through consideration of the key components of the MC mechanism, we have devised a novel, template-free method of synthesizing nanowires of quaternary and quinary metal oxides. By utilizing a high-temperature flux in the form of NaCl, we were able to fine-tune the MC mechanism, enabling the synthesis of nanowires of three different types of cuprate superconductors. This synthesis establishes a new generalized strategy for synthesizing nanowires without the necessity for a template or expensive lithographic techniques and could unlock cheaper methods of creating a wide range of metal oxide nanowires. Of key importance is that these methods result in straight-edged, crystalline wires which would be otherwise difficult to manufacture through bottom-up techniques.

4. Experimental Section

Syntheses: YBCO control experiments involved mixing stoichiometric amounts of yttrium oxide (Y_2O_3), copper oxide (CuO), and barium carbonate ($BaCO_3$), hand ground and pressed into a pellet using a 10 mm die and pressed to ≈ 2 tons for 10 min. This pellet was then broken up slightly and placed on the back of an alumina boat before heating to 920 °C for 2 h.

Barium carbonate nanoparticles were synthesized using either gel combustion^[21] or coprecipitation methods. For the latter, stock solutions of 0.05 M aqueous metal nitrates [$X(NO_3)_2$, $X = Ba$] and 0.025 M Na_2CO_3 were prepared, and 100 mL of the former solution was placed in a sonicator. Under sonication and vigorous stirring 200 mL of the 0.025 M solution was added dropwise over 8 h. The resultant milky solution was dried at 110 °C before being calcined at 450 °C. The resulting white powder was collected and analyzed.

For the template-free nanowire synthesis of Y123 and La123, stoichiometric amounts of Y_2O_3 in the case of Y123, or La_2O_3 in the case of La123, were combined with $BaCO_3$ nanoparticles and CuO. In addition, a NaCl flux was added at 10 wt%. All powders were hand-ground before being pressed into a pellet in the same manner as the Y123 control experiments. For Y123, the optimum dwell temperature was found to be 880 °C, and for La123 the optimum dwell temperature was found to be 820 °C.

Calcium copper acetate hexahydrate was synthesized via noncongruent crystallization. Calcium acetate monohydrate (3.55 g, 2.0 mol dm^{-3}) was dissolved in deionized water (10 mL at ≈ 70 °C). Separately, copper acetate monohydrate (1.00 g, 0.67 mol dm^{-3}) was dissolved in deionized water (7.5 mL at ≈ 70 °C). To ensure complete dissolution of the salts, further, water was added dropwise. The two solutions were subsequently mixed at 70 °C then filtered, covered, and allowed to stand until dark blue crystals formed. The resulting crystals were ball-milled for 24 h to attain a fine powder.

Bi-2201 was synthesized by a biopolymer-mediated synthesis. Bismuth nitrate pentahydrate (485.21 mg, 0.1 M), strontium nitrate (211.6 mg, 0.1 M), and copper nitrate hemi(pentahydrate) (232.6, 0.05 M) were added to 10 mL deionized water, along with (0.5 g) ethylenediaminetetraacetic acid and (300 μ L) ammonium. The solution was covered and then heated to 80 °C until all the metal salts were dissolved. This solution was subsequently transferred to a crucible, and dextran (5 g) was added. The material was stirred mechanically with a spatula, allowing a thick gel to form. The crucible was left in an oven at 80 °C overnight to allow all water to evaporate, before subsequent calcination at 850 °C with a ramp rate of 5 °C min^{-1} and a dwell time of 2 h.

Bi-2212 was synthesized by mixing Bi-2201 (39.10 mg $pellet^{-1}$, 0.0519 mmol $pellet^{-1}$) with one equivalent of $CaCu(CH_3COO)_4 \cdot 6H_2O$ (23.3 mg $pellet^{-1}$, 0.0519 mmol $pellet^{-1}$), and 30 mol% of NaCl (1.8 mg $pellet^{-1}$, 0.0312 mmol $pellet^{-1}$) relative to the bismuth content in Bi-2201. The mixture was then grounded by hand until the resulting powders appeared homogeneous in color and particle size was indeterminate by eye, ≈ 10 min. The mixture was then loaded into a 10 mm pellet die and pressed at 2 tons for a minimum of 10 min. The resulting pellets were gently broken to increase surface area, $\approx 4-8$ pieces per pellet, and were then calcined on an alumina surface at 850 °C for 2 h, with a heating rate of 5 °C min^{-1} .

Characterizations: SEM with EDX was carried out using JEOL IT300 SEM using an accelerating voltage of 15 kV. In a typical analysis, the sample was adhered to an aluminum stub with a conductive carbon sticker, and the sample was then either analyzed or coated with ≈ 10 nm carbon. TEM with EDX was carried out on a JEOL 1400 with an accelerating voltage of 120 kV. Nanowire samples were sonicated in ethanol for 10 s before casting onto a lacey carbon film. pXRD was carried out on a Bruker D8 Advance powder X-ray diffractometer with a Cu-K α ($\lambda = 1.5418$ Å) source and a positron-sensitive PSD LynxEye detector. Multiphase Rietveld refinement was carried out using the software Profex (version 5.0.2) to determine phase quantities and unit cell parameters. Profex provides a graphical user interface for the BGMN Rietveld refinement program.^[22] Variable temperature pXRD was carried out on a Bruker D8 Advance with Anton Parr heating stage, the X-ray source was a sealed tube with a copper anode, and the detector was a solid-state LynxEye position sensitive detector (PSD) with a 3° electronic window. The SQUID data for the bulk material were acquired by crushing the calcined pellets and placing them into a gel capsule. The samples were cooled under zero field, before the field was applied, and the moment was measured while the samples were warmed to obtain a zero-field cooled measurement. For Y123 and Bi2212, SQUID magnetometry was carried out on a quantum design MPMS VSM SQUID EverCool system. For La123, SQUID magnetometry was carried out on a quantum design MPMS 3 magnetometer.

Supporting Information

Supporting Information is available from the Wiley Online Library or from the author.

Acknowledgements

The authors would like to thank Natalie Pridmore and Jean-Charles Eloi for running pXRD and TEM experiments, respectively. S.R.H. would also like to thank Laurie Baxter and Alex Browning for their work on these systems as part of their undergraduate final-year research projects.

Conflict of Interest

The authors declare no conflict of interest.

Data Availability Statement

The data that support the findings of this study are available from the corresponding author upon reasonable request.

Keywords

flux growth, metal oxides, nanowires, superconductors, synthesis

Received: March 9, 2023

Revised: June 27, 2023

Published online:

-
- [1] Y. Cui, Z. Zhong, D. Wang, W. U. Wang, C. M. Lieber, *Nano Lett.* **2003**, *3*, 149.
- [2] C. K. Chan, H. Peng, G. Lui, K. McIlwrath, X. F. Zhang, R. A. Huggins, Y. Cui, *Nat. Nanotechnol.* **2008**, *3*, 31.
- [3] E. C. Garnett, P. Yang, *J. Am. Chem. Soc.* **2008**, *130*, 9224.
- [4] Y. Cui, Q. Wei, H. Park, C. M. Lieber, *Science* **2001**, *293*, 1289.
- [5] Z. L. Wang, J. Song, *Science* **2006**, *312*, 242.
- [6] M. Mashock, K. Yu, S. Cui, S. Mao, G. Lu, J. Chen, *ACS Appl. Mater. Interfaces* **2012**, *4*, 4192.
- [7] S. S. Shin, W. S. Yang, J. H. Noh, J. H. Suk, N. J. Jeon, J. H. Park, J. S. Kim, W. M. Seong, S. I. Seok, *Nat. Commun.* **2015**, *6*, 7410.
- [8] L. Ozyuzer, A. E. Koshelev, C. Kurter, N. Gopalsami, Q. Li, M. Tachiki, K. Kadowaki, T. Yamamoto, H. Minami, H. Yamaguchi, T. Tachiki, K. E. Gray, W.-K. Kwok, U. Welp, *Science* **2007**, *318*, 1291.
- [9] P. U. Jepsen, D. G. Cooke, M. Koch, *Laser Photon. Rev.* **2011**, *5*, 124.
- [10] R. Boston, Z. Schnepf, Y. Nemoto, Y. Sakka, S. R. Hall, *Science* **2014**, *344*, 623.
- [11] Z. A. C. Schnepf, S. Wimbush, S. Mann, S. R. Hall, *Adv. Mater.* **2008**, *20*, 1782.
- [12] Z. Schnepf, J. Mitchells, S. Mann, S. R. Hall, *Chem. Commun.* **2010**, *46*, 4887.
- [13] Z. Schnepf, S. Wimbush, S. Mann, S. R. Hall, *CrystEngComm.* **2010**, *12*, 1410.
- [14] R. S. Wagner, W. C. Ellis, *Appl. Phys. Lett.* **1964**, *4*, 89.
- [15] *CRC Handbook of Chemistry and Physics*, (Ed.: W. M. Haynes), 95th ed., CRC Press, Boca Raton, FL **2014**, pp. 4–89.
- [16] L. C. Pathak, S. K. Mishra, *Supercond. Sci. Technol.* **2005**, *18*, R67.
- [17] P. Badica, A. Agostino, M. M. R. Khan, S. Cagliero, C. Plapcianu, L. Pastero, M. Truccato, Y. Hayasaka, G. Jakob, *Supercond. Sci. Tech.* **2012**, *25*, 105003.
- [18] M. Klinger, *J. Appl. Cryst.* **2017**, *50*, 1226.
- [19] D. C. Green, R. Boston, S. Glatzel, M. R. Lees, S. C. Wimbush, J. Potticary, W. Ogasawara, S. R. Hall, *Adv. Funct. Mater.* **2015**, *25*, 4700.
- [20] O. G. Rojas, T. Nakayama, S. R. Hall, *Ceram. Int.* **2019**, *45*, 8546.
- [21] A. Zelati, A. Amirabadizadeh, A. Kompany, *Int. J. Chem. Eng. Appl.* **2011**, *2*, 299.
- [22] N. Doebelin, R. Kleeberg, *J. Appl. Crystallogr.* **2015**, *48*, 1573.